

Ligand Design

Photomechanical Actuation of Ligand Geometry in Enantioselective Catalysis**

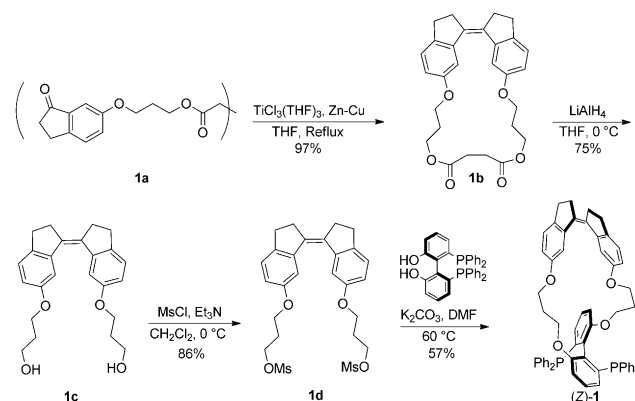
Zachary S. Kean, Sergey Akbulatov, Yancong Tian, Ross A. Widenhoefer,* Roman Boulatov,* and Stephen L. Craig*

Abstract: A catalyst that couples a photoswitch to the biaryl backbone of a chiral bis(phosphine) ligand, thus allowing photochemical manipulation of ligand geometry without perturbing the electronic structure is reported. The changes in catalyst activity and selectivity upon switching can be attributed to intramolecular mechanical forces, thus laying the foundation for a new class of catalysts whose selectivity can be varied smoothly and in situ over a useful range by controlling molecular stress experienced by the catalyst during turnover. Forces on the order of 100 pN are generated, thus leading to measurable changes in the enantioselectivities of asymmetric Heck arylations and Trost allylic alkylations. The differential coupling between applied force and competing stereochemical pathways is quantified and found to be more efficient for the Heck arylations.

“Switchable” catalytic systems have generated considerable interest because of their potential to trigger and/or optimize activity in situ with spatiotemporal control. This external modulation of chemical processes may benefit fields ranging from nanofabrication to biologically relevant therapeutics and diagnostics.^[1] Ultimately, such systems might enable otherwise inaccessible reactivity by switching between multiple active forms on the timescale of catalytic turnover^[1b] or polymer enchainment.^[2] A potentially useful, but heretofore untapped, trigger is the application of a mechanical force. Whereas mechanical force has been used to activate latent catalysts,^[3] it should also be capable of modulating an active catalyst, for example by distorting ligand geometry. As a first step toward that end, we sought a catalyst whose activity could be modulated^[4] (rather than turned on/off or reversed) externally, but through purely mechanical/geometric effects as opposed to electronic changes. Our design employs a stiff stilbene (1,1'-biindane) photoswitch which

offers good quantum efficiency, large geometry changes, molecular rigidity, and thermal stability.^[5] Stiff stilbenes have been used in light-driven molecular machines,^[6] including Feringa's rotor-based catalyst for photoswitchable asymmetric thiol-Michael additions.^[7] Additionally, the *Z* to *E* isomerization of stiff stilbene has been used to generate highly strained macrocycles which function as molecular force probes for quantitative studies of mechanochemical reactivity.^[8] Given this foundation, we set out to construct a ligand that was switchable between two states and would have differential reactivity,^[9] as has been well-characterized in the C_n-TunePhos ligands:^[10] a “compressed” state with a biaryl dihedral angle (ϕ ; see Scheme 2) which is more acute than that of the acyclic analogue (MeOBiphep, $\phi = 97^\circ$), and an “extended” state with a more obtuse dihedral angle.

Synthesis of the macrocyclic ligand (*Z*)-**1** (Scheme 1) proceeded using modifications of previously described procedures (see the Supporting Information).^[8b, 10b, 11] DFT cal-



Scheme 1. Synthesis of the photoswitchable chiral bisphosphine (*Z*)-**1**. DMF = *N,N*-dimethylformamide, Ms = methanesulfonyl, THF = tetrahydrofuran.

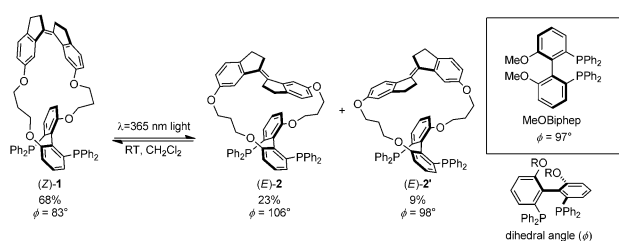
culations predict that (*Z*)-**1** is compressed ($\phi = 83^\circ$), (*E*)-**2** is extended ($\phi = 106^\circ$), and (*E*)-**2'** is virtually undistorted in terms of biaryl geometry ($\phi = 98^\circ$) relative to untethered MeOBiphep. The natural dihedral angle (as well as the related natural bite angle) of bis(phosphine) ligands is a geometric parameter commonly referenced in regard to catalyst selectivity.^[10b,c, 12] When irradiated at $\lambda = 365$ nm in dichloromethane, (*Z*)-**1** yielded a photostationary 68:23:9 (¹H NMR; see the Supporting Information) mixture of (*Z*)-**1**/*(E)*-**2**/*(E)*-**2'** within minutes (Scheme 2). Each isomer was isolated from the mixture using conventional flash or medium

[*] Z. S. Kean, Prof. R. A. Widenhoefer, Prof. S. L. Craig
Department of Chemistry, Duke University
French Family Science Center, Durham, NC 27708-0346 (USA)
E-mail: rwidenho@chem.duke.edu
stephen.craig@duke.edu

Dr. S. Akbulatov, Dr. Y. Tian, Dr. R. Boulatov
Department of Chemistry, University of Liverpool
Crown Street, Liverpool, L69 7ZD (UK)
E-mail: r.boulatov@liv.ac.uk

[**] This work was supported by the Army Research Office (W-911-NF-1110071 to S.L.C. and R.A.W.) and by an EPSRC Early Career Fellowship to R.B. Computational resources were provided by XSEDE (TG-CHE140039 and TG-CHE130071).

Supporting information for this article is available on the WWW under <http://dx.doi.org/10.1002/anie.201407494>.



Scheme 2. Irradiation of (*Z*)-**1** at $\lambda = 365$ nm generates a photostationary mixture (given as %) of (*Z*)-**1**, (*E*)-**2**, (*E*)-**2'**. (*E*)-**2** and (*E*)-**2'** are isolable diastereomers because of the combination of atropisomerism in the tethered stiff stilbene and fixed chirality of the bis(phosphine). (*Z*)-**1** also exists as a pair of diastereomers (effectively diastereomeric conformers) that are unresolvable because of the low barrier for isomerization across the alkene (ca. 6 kcal mol⁻¹ in untethered *Z*-stiff stilbene^[8d]). Distortion of ligand geometry is evaluated using the calculated (DFT) “natural” dihedral angle (ϕ) defined by the biaryl carbons at the positions shown in bold (bottom right). All ligands used in this study are axially chiral about the biaryl backbone in the *S* configuration.

pressure liquid chromatography, thus allowing further study of pure (*Z*)-**1** and (*E*)-**2**. When embedded in a macrocycle, *E* stiff stilbenes assume axial chirality, such that both (*E*)-**2** and (*E*)-**2'** are diastereomers of atropisomers. X-ray crystallography of the derivative phosphine selenides of (*E*)-**2** and (*Z*)-**1** confirmed the stereochemistry of all three isomers and the expected greater dihedral angle in (*E*)-**2** relative to that in (*Z*)-**1** (see the Supporting Information).

The isolated ligands were employed in the asymmetric Heck reaction between 2,3-dihydrofuran (DHF) and either phenyl^[13] or 1-naphthyl^[14] triflate to form 2-aryl dihydrofurans. In the case of arylation with phenyl triflate (Table 1, entries 1–3), (*E*)-**2** yields **3a** in 79% *ee* (e.r. = 89:11; GC) and high conversion (GC, 95%), whereas the distortion in ϕ in (*Z*)-**1** yields **3a** in 96% *ee* (e.r. = 98:2) (Figure 1a) and 55% conversion. Here, the stretched ligand (*E*)-**2** results in a decreased enantioselectivity relative to the acyclic MeOBiphep (90% *ee*), while the compressed ligand (*Z*)-**1** exhibits higher selectivity. In contrast to prior photoswitchable

Table 1: Summary of ligand screen in the asymmetric Heck reaction of phenyl triflate and 2,3-dihydrofuran.^[a]

Entry	Ligand	Conv. [%] ^[b]	3a/4a ^[c]	Total (<i>S</i>) products [%]	(<i>S</i>)- 3a <i>ee</i> [%] ^[d]
1	MeOBiphep	23	95:5	91	90
2	(<i>Z</i>)- 1	55	97:3	96	96
3	(<i>E</i>)- 2	95	98:2	88	79
4 ^[e]	(<i>E</i>)- 2 + 365 nm	93	97:3	93	90

[a] Reaction carried out using phenyl triflate (1 equiv, 0.6 M), ligand (0.06 equiv), Pd(OAc)₂ (0.03 equiv), 2,3-DHF (5.6 equiv), *i*Pr₂NEt (3.4 equiv) in benzene at 40 °C for 24 h. All values are averages of duplicate runs. [b,c] Determined by GC. [d] Determined by GC on chiral stationary phase (Supelco β -Dex). Absolute configuration determined by comparison with sign of optical rotation as previously reported.^[13a,17] Tf = trifluoromethanesulfonyl.

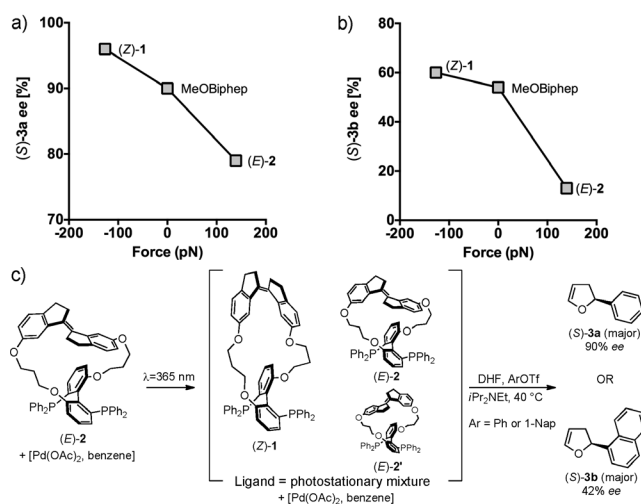


Figure 1. The *ee* value of (*S*)-**3a** (a) and (*S*)-**3b** (b) as a function of force for ligands used in this study. c) Irradiation of catalyst solution in situ at $\lambda = 365$ nm yields a presumed photostationary mixture of ligands, thus changing the selectivity in asymmetric Heck arylations.

cataysts,^[4] (*Z*)-**1** and (*E*)-**2** differ in their shape but not their electronics (σ -donating ability) at the phosphorus atoms, as indicated by the identical ³¹P–⁷⁷Se coupling constants (¹*J*_{P,Se}, both 739 Hz) of the corresponding phosphine selenides^[15] and supported by a comparison with the *C_n*-TunePhos ligands (see the Supporting Information).^[10c,16] This evidence suggests that geometric/steric effects predominate, and that the contribution of the stiff stilbene moiety can be considered from a purely mechanical point of view.

For arylation with 1-naphthyl triflate, qualitatively similar effects are observed (Table 2), with (*Z*)-**1** yielding **3b** in 60% *ee* (HPLC), versus only 13% *ee* from (*E*)-**2**. Both reactions proceed to high conversion (*ee* is independent of conversion; see the Supporting Information), although, in contrast to the reaction with phenyl triflate, ligand distortion now has a substantial impact on regioselectivity [for (*E*)-**2**, **3b/4b** = 88:12; for (*Z*)-**1**, **3b/4b** = 72:28; Figure 1b]. The selectivity of Heck arylations has been attributed to two

Table 2: Summary of ligand screen in the asymmetric Heck reaction of 1-naphthyl triflate and 2,3-dihydrofuran.^[a]

Entry	Ligand	Conv. [%] ^[b]	3b/4b ^[c]	Total (<i>S</i>) products [%] ^[d]	(<i>S</i>)- 3b <i>ee</i> [%] ^[d]
1	MeOBiphep	98	79:21	64	54
2	(<i>Z</i>)- 1	91	72:28	63	60
3	(<i>E</i>)- 2	> 99	88:12	52	13
4	(<i>E</i>)- 2 + 365 nm	> 99	85:15	69	42

[a] Reaction carried out using 1-naphthyl triflate (1 equiv, 0.6 M), ligand (0.06 equiv), Pd(OAc)₂ (0.03 equiv), 2,3-DHF (5.6 equiv), *i*Pr₂NEt (3.4 equiv) in benzene at 40 °C for 24 h. [b,c] Determined by GC [d] Determined by HPLC on chiral stationary phase (Daicel CHIRALPAK AD-H) and GC on normal stationary phase (see the Supporting Information). Absolute configuration determined by comparison with sign of optical rotation as previously reported.^[14]

sequential processes:^[13] the initial irreversible insertion of DHF at C2 into the Pd–aryl bond (which determines the total *S/R* ratio at C2 in all regioisomers), and then the isomerization and regiodetermining displacement of the metal to generate either the 2,3- or 2,5-DHF product. Here, as the natural dihedral angle of the ligand increases, selectivity of the initial enantiodiscriminating step decreases, as reflected in an overall decrease in the percentage of (*S*)-**3b** + (*S*)-**4b** is obtained. Further, the wider dihedral angle slows ligand displacement to form (*S*)-**3b** or accelerates the insertion/ β -hydride elimination processes which lead to isomerization and formation of the 2,3-dihydrofuran isomers **3**, as evidenced by the greater total content of **3** (both enantiomers) relative to that of **4** with increasing ligand dihedral angle. In contrast to the Heck arylations examined, Trost allylic alkylations using standard substrates (Table 3) showed more modest changes in selectivity between the ligands *Z*-(**1**) and *E*-(**2**), thus demonstrating a lower sensitivity to the forces or geometric changes which we are able to achieve by photo-mechanical actuation.

Table 3: Summary of ligand screen in Trost asymmetric allylic alkylations.^[a]

Entry	Ligand	Yield [%] ^[b]	Product	<i>ee</i> [%]
1	MeOBiphep	98	(<i>R</i>)- 5a ^[c]	93 ^[d]
2	(<i>Z</i>)- 1	95	(<i>R</i>)- 5a ^[c]	93 ^[d]
3	(<i>E</i>)- 2	96	(<i>R</i>)- 5a ^[c]	91 ^[d]
4	MeOBiphep	96	5b	37 ^[e]
5	(<i>Z</i>)- 1	92	5b	45 ^[e]
6	(<i>E</i>)- 2	96	5b	40 ^[e]

[a] Reaction carried out using allyl acetate (1 equiv, 0.2 M), ligand (0.05 equiv), [$\text{Pd}(\text{allyl})\text{Cl}$]₂ (0.025 equiv), dimethyl malonate (3 equiv), BSA (3 equiv), and KOAc (cat.) in CH₂Cl₂ at RT for 20 h. [b] Yield of product isolated after column chromatography. [c] Absolute configuration determined by comparison with sign of optical rotation as previously reported.^[20] [d] Determined by HPLC on chiral stationary phase (Daicel CHIRALPAK AD-H). [e] Determined by ¹H NMR spectroscopy with [Eu(hfc)₃] chiral shift reagent. Absolute configuration not determined. BSA = bis(trimethylsilyl)acetamide.

Importantly, the changes in reactivity are a consequence of an applied mechanical distortion, and the relevant forces can be quantified. Following previously described methodology,^[8a,18] DFT calculations at the B3LYP/6-311 + G(d) level of theory on complete conformational ensembles of MeOBiphep, with constraining potential imposed across the C atoms of the Me groups, yielded a calibration curve which relates the O...O bond distance to the force applied to adjacent carbon atoms (indicated by arrows in Figure 2) for (*Z*)-**1**, (*E*)-**2**, and (*E*)-**2'**. The O...O distance was chosen because it best represents the pulling coordinate through which the dihedral angle is compressed or widened by stiff stilbene. This approach has been validated previously^[8a] against single-molecule force spectroscopy data^[19] in the context of *gem*-dibromocyclopropane ring opening. As summarized in Table 4, the compression of the dihedral angle in (*Z*)-**1** to

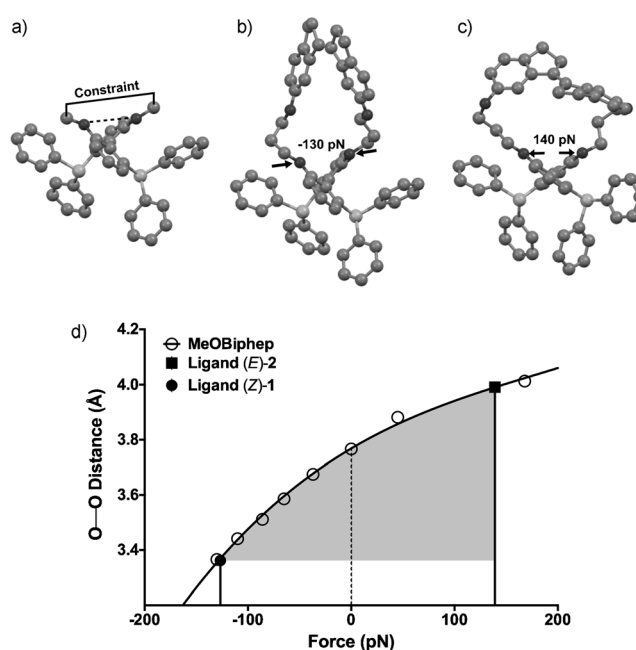


Figure 2. a) Constraint applied to terminal methyl groups on MeOBiphep generates a calibration curve (solid curve in d) of O...O distance (dashed line) versus force. Calibration yields a compressive force of –130 pN and an extensional force of 140 pN for (*Z*)-**1** (b) and (*E*)-**2** (c), respectively. d) Calculated O...O distance of (*Z*)-**1** and (*E*)-**2** plotted on MeOBiphep calibration curve yields force values. Shaded area illustrates the work done along the O...O between (*Z*)-**1** and (*E*)-**2**.

Table 4: Summary of geometric and force parameters of ligands used in this study.

Ligand	Photostationary content [%]	Dihedral angle [ϕ]	O...O distance [Å]	Force [pN] ^[a]
MeOBiphep	–	97	3.77	0
(<i>Z</i>)- 1	68	83	3.36	–130
(<i>E</i>)- 2	23	106	3.99	140
(<i>E</i>)- 2'	9	98	3.74	–14

[a] Negative sign corresponds to compressive force.

83° requires the equivalent of 130 pN of compressive force applied to MeOBiphep, whereas the extension of the dihedral angle of (*E*)-**2** to 106° would be observed if a tensile load of 140 pN were applied in the opposite direction. The highest energy isomer, (*E*)-**2'**, shows negligible distortion along the O...O coordinate, a minimal compressive force (14 pN), and only 1° distortion about the dihedral angle relative to MeOBiphep, thus illustrating that even in such fairly small molecules the local restoring force is a better predictor of reactivity than strain energy.^[5,8b,d] The magnitude of these forces provides a first benchmark for the design and implementation of catalysts and catalyst platforms which are mechanically tunable and/or switchable in situ. Interestingly, although secondary to our purposes, photoswitching also occurs in the presence of Pd(OAc)₂ in benzene (Figure 1 c). Irradiating (*E*)-**2** ($\lambda = 365$ nm, 3 W, 60 s) presumably gives a photostationary mixture of isomers, and the ensuing Heck reactions proceed with a selectivity which is intermediate to that of (*E*)-**2** and (*Z*)-**1** (Figure 1 a,b).

Looking ahead, we note that the forces required to effect significant perturbation of the dihedral angle of (*Z*)-**1** and (*E*)-**2** ($\Delta\phi = 23^\circ$) are small relative to those necessary to trigger covalent chemistry in many mechanophores whose activity has been previously characterized.^[21] In particular, similar forces (<500 pN) are believed to be operative in the mechanically driven ring-opening reaction of spiropyran to merocyanine on the time scale of seconds,^[22] and so the forces demonstrated here are directly relevant to those experienced by molecules in a range of material platforms.^[23] In such materials, the MeOBiphep-based catalysts, and other modulated mechanocatalysts might therefore provide an amplified chemical response to localized stress and/or access to new reversibly tunable reactions. Materials and soft devices in which the necessary forces can be generated reversibly and repeatedly^[24] are especially attractive in this regard, because of the potential to toggle between multiple active forms of the same catalyst.

Received: July 22, 2014

Revised: September 18, 2014

Published online: October 30, 2014

Keywords: density functional calculations · homogeneous catalysis · ligand design · photochemistry · P ligands

- [1] a) B. M. Neilson, C. W. Bielawski, *ACS Catal.* **2013**, *3*, 1874–1885; b) R. S. Stoll, S. Hecht, *Angew. Chem. Int. Ed.* **2010**, *49*, 5054–5075; *Angew. Chem.* **2010**, *122*, 5176–5200; c) R. Göstl, A. Senf, S. Hecht, *Chem. Soc. Rev.* **2014**, *43*, 1982–1996.
- [2] a) B. P. Fors, C. J. Hawker, *Angew. Chem. Int. Ed.* **2012**, *51*, 8850–8853; *Angew. Chem.* **2012**, *124*, 8980–8983; b) B. M. Neilson, C. W. Bielawski, *Chem. Commun.* **2013**, *49*, 5453–5455.
- [3] a) A. Piermattei, S. Karthikeyan, R. P. Sijbesma, *Nat. Chem.* **2009**, *1*, 133–137; b) R. Groote, R. T. M. Jakobs, R. P. Sijbesma, *Polym. Chem.* **2013**, *4*, 4846–4859; c) A. G. Tennyson, K. M. Wiggins, C. W. Bielawski, *J. Am. Chem. Soc.* **2010**, *132*, 16631–16636.
- [4] a) D. Sud, T. B. Norsten, N. R. Branda, *Angew. Chem. Int. Ed.* **2005**, *44*, 2019–2021; *Angew. Chem.* **2005**, *117*, 2055–2057; b) D. Sud, R. McDonald, N. R. Branda, *Inorg. Chem.* **2005**, *44*, 5960–5962.
- [5] Z. Huang, R. Boulatov, *Chem. Soc. Rev.* **2011**, *40*, 2359–2384.
- [6] N. Koumura, R. W. J. Zijlstra, R. A. van Delden, N. Harada, B. L. Feringa, *Nature* **1999**, *401*, 152–155.
- [7] J. B. Wang, B. L. Feringa, *Science* **2011**, *331*, 1429–1432.
- [8] a) S. Akbulatov, Y. C. Tian, R. Boulatov, *J. Am. Chem. Soc.* **2012**, *134*, 7620–7623; b) T. J. Kucharski, Z. Huang, Q. Z. Yang, Y. C. Tian, N. C. Rubin, C. D. Concepcion, R. Boulatov, *Angew. Chem. Int. Ed.* **2009**, *48*, 7040–7043; *Angew. Chem.* **2009**, *121*, 7174–7177; c) Y. C. Tian, T. J. Kucharski, Q. Z. Yang, R. Boulatov, *Nat. Commun.* **2013**, *4*, 2538; d) Q. Z. Yang, Z. Huang, T. J. Kucharski, D. Khvostichenko, J. Chen, R. Boulatov, *Nat. Nanotechnol.* **2009**, *4*, 302–306; e) T. J. Kucharski, Q. Z. Yang, Y. C. Tian, R. Boulatov, *J. Phys. Chem. Lett.* **2010**, *1*, 2820–2825.
- [9] a) B. M. Trost, D. L. VanVranken, *Chem. Rev.* **1996**, *96*, 395–422; b) B. M. Trost, D. L. Van Vranken, C. Bingel, *J. Am. Chem. Soc.* **1992**, *114*, 9327–9343; c) B. M. Trost, J. L. Zambrano, W. Richter, *Synlett* **2001**, 907–909.
- [10] a) W. J. Tang, X. M. Zhang, *Chem. Rev.* **2003**, *103*, 3029–3069; b) Z. G. Zhang, H. Qian, J. Longmire, X. M. Zhang, *J. Org. Chem.* **2000**, *65*, 6223–6226; c) M. Raghunath, X. Zhang, *Tetrahedron Lett.* **2005**, *46*, 8213–8216.
- [11] L. Q. Qiu, F. Y. Kwong, J. Wu, W. H. Lam, S. Chan, W. Y. Yu, Y. M. Li, R. W. Guo, Z. Zhou, A. S. C. Chan, *J. Am. Chem. Soc.* **2006**, *128*, 5955–5965.
- [12] a) P. Dierkes, P. van Leeuwen, *J. Chem. Soc. Dalton Trans.* **1999**, 1519–1529; b) P. W. N. M. van Leeuwen, P. C. J. Kamer, J. N. H. Reek, P. Dierkes, *Chem. Rev.* **2000**, *100*, 2741–2770; c) S. Jeulin, S. D. de Paule, V. Ratovelomanana-Vidal, J. P. Genet, N. Champion, P. Dellis, *Proc. Natl. Acad. Sci. USA* **2004**, *101*, 5799–5804.
- [13] a) F. Ozawa, A. Kubo, T. Hayashi, *Tetrahedron Lett.* **1992**, *33*, 1485–1488; b) D. Mc Cartney, P. J. Guiry, *Chem. Soc. Rev.* **2011**, *40*, 5122–5150.
- [14] O. Loiseleur, M. Hayashi, N. Schmees, A. Pfaltz, *Synthesis* **1997**, 1338–1345.
- [15] a) D. W. Allen, B. F. Taylor, *J. Chem. Soc. Dalton Trans.* **1982**, 51–54; b) N. G. Andersen, M. Parvez, B. A. Keay, *Org. Lett.* **2000**, *2*, 2817–2820; c) A. Suárez, M. A. Méndez-Rojas, A. Pizzano, *Organometallics* **2002**, *21*, 4611–4621; d) S. Jeulin, S. Duprat de Paule, V. Ratovelomanana-Vidal, J.-P. Genêt, N. Champion, P. Dellis, *Angew. Chem. Int. Ed.* **2004**, *43*, 320–325; *Angew. Chem.* **2004**, *116*, 324–329.
- [16] X. Zhang, US 6,521,769 B1, **2003**.
- [17] E. Gorobets, M. Parvez, B. M. M. Wheatley, B. A. Keay, *Can. J. Chem.* **2006**, *84*, 93–98.
- [18] M. Hermes, R. Boulatov, *J. Am. Chem. Soc.* **2011**, *133*, 20044–20047.
- [19] D. Wu, J. M. Lenhardt, A. L. Black, B. B. Akhremitchev, S. L. Craig, *J. Am. Chem. Soc.* **2010**, *132*, 15936–15938.
- [20] M. Yamaguchi, T. Shima, T. Yamagishi, M. Hida, *Tetrahedron Lett.* **1990**, *31*, 5049–5052.
- [21] M. T. Ong, J. Leiding, H. L. Tao, A. M. Virshup, T. J. Martinez, *J. Am. Chem. Soc.* **2009**, *131*, 6377–6379.
- [22] M. N. Silberstein, K. Min, L. D. Creumar, C. M. Degen, T. J. Martinez, N. R. Aluru, S. R. White, N. R. Sottos, *J. Appl. Phys.* **2013**, *114*, 023504.
- [23] a) B. A. Beiermann, D. A. Davis, S. L. B. Kramer, J. S. Moore, N. R. Sottos, S. R. White, *J. Mater. Chem.* **2011**, *21*, 8443–8447; b) C. K. Lee, D. A. Davis, S. R. White, J. S. Moore, N. R. Sottos, P. V. Braun, *J. Am. Chem. Soc.* **2010**, *132*, 16107–16111; c) S. L. Potisek, D. A. Davis, N. R. Sottos, S. R. White, J. S. Moore, *J. Am. Chem. Soc.* **2007**, *129*, 13808–13809; d) C. M. Kingsbury, P. A. May, D. A. Davis, S. R. White, J. S. Moore, N. R. Sottos, *J. Mater. Chem.* **2011**, *21*, 8381–8388.
- [24] a) M. B. Larsen, A. J. Boydston, *J. Am. Chem. Soc.* **2014**, *136*, 1276–1279; b) G. R. Gossweiler, G. B. Hewage, G. Soriano, Q. Wang, G. W. Welshofer, X. Zhao, S. L. Craig, *ACS Macro Lett.* **2014**, *3*, 216–219.